



**University of  
Zurich** UZH

**Zurich Open Repository and  
Archive**

University of Zurich  
University Library  
Strickhofstrasse 39  
CH-8057 Zurich  
[www.zora.uzh.ch](http://www.zora.uzh.ch)

---

Year: 2023

---

## **Relationship between magnetic resonance imaging findings and histological grade in spinal peripheral nerve sheath tumors in dogs**

Morabito, Simona ; Specchi, Swan ; Di Donato, Pamela ; Pollard, Danica ; Dennis, Ruth ; De Risio, Luisa ; Bacon, Nicholas J ; Potamopoulou, Maria ; Rupp, Stefan ; Corlazzoli, Daniele ; Ribeiro, João ; Cozzi, Francesca ; Jurina, Konrad ; Cappello, Rodolfo ; Mercuriali, Edy ; Beckmann, Katrin ; Flegel, Thomas ; Menchetti, Marika ; König, Florian ; Matiassek, Kaspar ; Rosati, Marco

DOI: <https://doi.org/10.1111/jvim.16839>

Posted at the Zurich Open Repository and Archive, University of Zurich

ZORA URL: <https://doi.org/10.5167/uzh-253796>

Journal Article

Published Version









The following work is licensed under a Creative Commons: Attribution-NonCommercial-NoDerivatives 4.0 International (CC BY-NC-ND 4.0) License.

Originally published at:

Morabito, Simona; Specchi, Swan; Di Donato, Pamela; Pollard, Danica; Dennis, Ruth; De Risio, Luisa; Bacon, Nicholas J; Potamopoulou, Maria; Rupp, Stefan; Corlazzoli, Daniele; Ribeiro, João; Cozzi, Francesca; Jurina, Konrad; Cappello, Rodolfo; Mercuriali, Edy; Beckmann, Katrin; Flegel, Thomas; Menchetti, Marika; König, Florian; Matiassek, Kaspar; Rosati, Marco (2023). Relationship between magnetic resonance imaging findings and histological grade in spinal peripheral nerve sheath tumors in dogs. *Journal of Veterinary Internal Medicine*, 37(6):2278-2290.

DOI: <https://doi.org/10.1111/jvim.16839>

# Relationship between magnetic resonance imaging findings and histological grade in spinal peripheral nerve sheath tumors in dogs

Simona Morabito<sup>1,2,3</sup>  | Swan Specchi<sup>1,3</sup> | Pamela Di Donato<sup>1,3</sup> |  
 Danica Pollard<sup>4</sup> | Ruth Dennis<sup>2,5</sup> | Luisa De Risio<sup>6</sup>  | Nicholas J. Bacon<sup>7</sup> |  
 Maria Potamopoulou<sup>7</sup> | Stefan Rupp<sup>8</sup> | Daniele Corlazzoli<sup>9,10</sup> | João Ribeiro<sup>11</sup>  |  
 Francesca Cozzi<sup>12</sup> | Konrad Jurina<sup>13</sup> | Rodolfo Cappello<sup>14</sup> | Edy Mercuriali<sup>15</sup> |  
 Katrin Beckmann<sup>16</sup>  | Thomas Flegel<sup>17</sup>  | Marika Menchetti<sup>18</sup> |  
 Florian König<sup>19</sup> | Kaspar Matiasek<sup>20</sup> | Marco Rosati<sup>20</sup> 

<sup>1</sup>Diagnostic Imaging Department, Veterinary Hospital "I Portoni Rossi" Anicura Italy, Zola Predosa, Bologna, Italy

<sup>2</sup>Animal Health Trust, Lanwades Park, Kentford, Newmarket, Suffolk, United Kingdom

<sup>3</sup>Antech Imaging Services, Irvine, California, USA

<sup>4</sup>British Horse Society, Kenilworth, Warwickshire, United Kingdom

<sup>5</sup>Dick White Referrals, Six Mile Bottom, Cambridgeshire CB8 0UH, United Kingdom

<sup>6</sup>Linnaeus Veterinary Ltd, Friars Gate, Shirley, United Kingdom

<sup>7</sup>Fitzpatrick Referrals Oncology and Soft Tissue Ltd, Surrey, United Kingdom

<sup>8</sup>Small Animal Hospital Hofheim, IVC Evidensia, Munich, Germany

<sup>9</sup>Policlinico Veterinario Roma Sud, Rome, Italy

<sup>10</sup>Gregorio Settimo, Rome, Italy

<sup>11</sup>Faculdade de Medicina Veterinária da Universidade Lusófona de Humanidades e Tecnologias, Lisbon, Portugal

<sup>12</sup>Clinica Neurologica Veterinaria NVA, Milan, Italy

<sup>13</sup>AniCura Tierklinik Haar, Haar, Germany

<sup>14</sup>North Downs Specialist Referrals, Bletchingley, United Kingdom

## Abstract

**Background:** Peripheral nerve sheath tumors (PNSTs) are a group of neoplasms originating from Schwann cells or pluripotent cell of the neural crest. Therapeutic options and prognosis are influenced by their degree of malignancy and location.

**Hypothesis/Objectives:** Identify magnetic resonance imaging (MRI) features predictive of PNST histologic grade.

**Animals:** Forty-four dogs with histopathological diagnosis of spinal PNSTs and previous MRI investigation.

**Methods:** A multicenter retrospective study including cases with (a) histopathologic diagnosis of PNST and (b) MRI studies available for review. Histologic slides were reviewed and graded by a board-certified pathologist according to a modified French system (FNCLCC) for grading soft tissue sarcomas. The MRI studies were reviewed by 2 board-certified radiologists blinded to the grade of the tumor and the final decision on the imaging characteristics was reached by consensus. Relationships between tumor grade and histological and MRI findings were assessed using statistical analysis.

**Results:** Forty-four cases met inclusion criteria; 16 patients were PNSTs Grade 1 (low-grade), 19 were PNSTs Grade 2 (medium-grade), and 9 were PNSTs Grade 3 (high-grade). Large volume ( $P = .03$ ) and severe peripheral contrast enhancement ( $P = .04$ ) were significantly associated with high tumor grade. Degree of muscle

**Abbreviations:** BPNSTs, benign peripheral nerve sheath tumors; FLAIR, fluid-attenuated inversion recovery; FNCLCC, Fédération Nationale des Centres de Lutte Contre Le Cancer; FOV, field of view; GFAP, glial fibrillary acidic protein; H&E, hematoxylin-eosin; IQR, interquartile range; MPNSTs, malignant peripheral nerve sheath tumors; MRI, magnetic resonance imaging; PNSTs, peripheral nerve sheath tumors; ROI, region of interest; SMA, smooth muscle actin; STIR, short tau inversion recovery; SWI, susceptibility weighted imaging; W, weighted.

This is an open access article under the terms of the [Creative Commons Attribution-NonCommercial-NoDerivs](https://creativecommons.org/licenses/by-nc-nd/4.0/) License, which permits use and distribution in any medium, provided the original work is properly cited, the use is non-commercial and no modifications or adaptations are made.

© 2023 The Authors. *Journal of Veterinary Internal Medicine* published by Wiley Periodicals LLC on behalf of American College of Veterinary Internal Medicine.

<sup>15</sup>Centro Traumatologico Ortopedico Veterinario, Arenzano, Genoa, Liguria, Italy

<sup>16</sup>Neurology Service, Department of Small Animal Surgery, Vetsuisse Faculty, University of Zurich, Zürich, Switzerland

<sup>17</sup>Department of Small Animals, Faculty for Veterinary Medicine, University Leipzig, Leipzig, Germany

<sup>18</sup>Neurology and Neurosurgery Division, San Marco Veterinary Clinic, Veggiano, Padua, Italy

<sup>19</sup>Small Animal Practice, Neurology, Wiesbaden, Germany

<sup>20</sup>Section of Clinical & Comparative Neuropathology, Centre for Clinical Veterinary Medicine, Ludwig-Maximilians-Universität München, Munich, Germany

#### Correspondence

Marco Rosati, Section of Clinical & Comparative Neuropathology, Center for Clinical Veterinary Medicine, Ludwig-Maximilians-Universität München, Munich, Germany

Email: [marco.rosati@outlook.de](mailto:marco.rosati@outlook.de)

atrophy, heterogeneous signal and tumor growth into the vertebral canal were not associated with grade.

**Conclusions and Clinical Importance:** Grade of malignancy was difficult to identify based on diagnostic imaging alone. However, some MRI features were predictive of high-grade PNSTs including tumor size and peripheral contrast enhancement.

#### KEYWORDS

canine, magnetic resonance imaging, neoplasia, nerve root, neurofibroma, schwannoma, tumor grading

## 1 | INTRODUCTION

Primary neoplasms of the peripheral nervous system in dogs represent 26% of nervous system tumors in dogs.<sup>1</sup> Peripheral nerve sheath tumors (PNSTs) are a group of neoplasms originating from either Schwann cells, modified Schwann cells, intraneural fibroblasts, or perineural cells.<sup>2,3</sup> They typically exhibit endoneurial longitudinal spread, which is distinct from the transperineurial growth pattern of nonneural tumors that might only occasionally encase and efface peripheral nerves.<sup>4</sup> The latest edition of the World Health Organization (WHO) Classification of Tumors, published in 2021,<sup>5</sup> groups the cranial and paraspinal nerve tumors together with tumors of the central nervous system listing benign entities (BPNSTs) such as neurofibroma, schwannoma, and perineuroma and malignant tumors, called malignant PNST (MPNSTs).

Peripheral nerve sheath tumors of low (BPNST) and high (MPNST) grades have been observed in both cranial and spinal nerves in the dogs.<sup>6,7</sup> Histologically, the most reliable indicators of malignancy are high mitotic index, necrosis within the neoplasm and transperineurial growth. Benign peripheral nerve sheath tumors have a low mitotic index, even in densely cellular areas, whereas MPNSTs exceed 4 mitotic figures per 10 high-power fields. Nuclear morphology and hemorrhages are also increasingly associated with malignancy.<sup>4,7</sup>

Surgical resection and radiotherapy are currently the main therapeutic strategies for these tumors.<sup>8</sup> Unfortunately, these options are often not feasible by the time a diagnosis is made, particularly in the MPNST, because these tumors tend to invade the surrounding tissue, consistently infiltrating multiple nerve roots, plexus branches, and potentially the spinal cord or brainstem.<sup>9</sup>

Given that MPNSTs commonly invade and breach the epineurium of the affected nerves,<sup>10,11</sup> a higher recurrence rate after surgical resection is expected in dogs because of incomplete resection.<sup>12</sup> In people, the only

effective treatment for MPNST is complete surgical resection to obtain negative surgical margins; patients with negative margins have a relatively higher survival rate than those with positive margins.<sup>13</sup>

Previous reports described the imaging findings and outcome of PNSTs in small cohorts of dogs.<sup>14,15</sup> Despite accurate spatial resolution, imaging techniques cannot definitively support a clinical diagnosis of PNST.<sup>14-18</sup> Differential diagnoses include other tumors, such as meningioma in the intradural compartment,<sup>19</sup> lymphoma and sarcomas, or inflammatory lesions such as focal hypertrophic neuritis<sup>20,21</sup> and chronic hypertrophic ganglioneuritis,<sup>22</sup> all presenting with comparable imaging findings.

Despite its lack of specificity, magnetic resonance imaging (MRI) is the diagnostic modality of choice to diagnose PNSTs,<sup>15</sup> presumptively, because it allows for non-invasive early visualization of this entity.<sup>23-25</sup>

The frequent occurrence of malignant behavior in dogs emphasizes the importance of predicting the histologic grade of the tumors in pre-surgical settings. In veterinary medicine, few studies<sup>14,15</sup> have described imaging findings on computed tomography (CT) and MRI in small cohorts of dogs without investigating possible associations with histologic phenotype.

Our objective was to assess MRI findings of a large group of dogs with a tailored histologic classification and grading for PNSTs to identify imaging features predictive of their malignancy.

## 2 | MATERIALS AND METHODS

### 2.1 | Case selection criteria

Ours was a multicenter, retrospective, observational study, approved by the Research Ethics Committee of the Animal Health Trust (Ref19/2019).

**TABLE 1** Modified histological grading according to a modified French system (Fédération Nationale des Centres de Lutte Contre Le Cancer, FNCLCC) and additional features recorded for comparative analysis of histologic and MRI findings.

<b>Tumor differentiation</b>	
Score 1	Closely resembling normal tissue
Score 2	Histological typing is certain
Score 3	Embryonal or undifferentiated sarcomas
<b>Mitotic count (per 2.37 mm<sup>2</sup>)</b>	
Score 1	0-9 mitoses per 2.37 mm <sup>2</sup>
Score 2	10-19 mitoses per 2.37 mm <sup>2</sup>
Score 3	>19 mitoses per 2.37 mm <sup>2</sup>
<b>Tumor necrosis</b>	
Score 0	No necrosis
Score 1	<50% tumor necrosis
Score 2	≥50% tumor necrosis
<b>Histological grade</b>	Grade 1: total score 2, 3 Grade 2: total score 4, 5 Grade 3: total score 6, 7, 8
<b>Additional histologic features</b>	
<b>Hemorrhage</b>	
Score 0	Absent
Score 1	<50% of tumor area
Score 2	>50% of tumor area
<b>Stroma</b>	
Score 1	Delicate
Score 2	Moderate
Score 3	Abundant
<b>Myxoid changes</b>	
Score 0	Absent
Score 1	<50% of tumor area
Score 2	>50% of tumor area
<b>Cystic Changes</b>	
Score 0	Absent
Score 1	<50% of tumor area
Score 2	>50% of tumor area
<b>Mineralization</b>	
Score 0	Absent
Score 1	Present
<b>Inflammation</b>	
Score 0	Absent
Score 1	Mild
Score 2	Moderate
<b>Pigments</b>	
Score 0	Absent
Score 1	Present
<b>Margins</b>	
Negative	Free
Positive	Infiltrated

(Continues)

**TABLE 1** (Continued)

<b>Additional histologic features</b>	
<b>Epineurial Invasion</b>	
Score 0	Absent
Score 1	Present

Pathology reports of dogs diagnosed with PNSTs submitted between 2010 and 2020 were retrieved from the archive of the comparative neuropathology service of the Ludwig Maximilians Universität of Munich and the histopathological slides of the cases were reviewed by 2 neuropathologists (KM, MR).

Medical records and MR images of dogs with histologically confirmed PNST were collected from referral centers and multiple institutes. All animals were referred for investigation of neurologic problems, and previous informed written consent for research was obtained from all dog owners at time of biopsy submission and MRI investigation.

The inclusion criteria included (a) presence of a tumor involving a major peripheral nerve, plexus, or nerve root and fitting the histological criteria for PNSTs in dogs<sup>4,7</sup>; and (b) both histology slides and MR images needed to be available for review.

## 2.2 | Medical record review

Medical records were compiled and reviewed by the primary author (SM). Signalment, clinical history, clinical examination, neurological examination, age at the time of MRI, reason for performing MRI and final diagnosis, site of the MRI, surgery and biopsy results were recorded. Imaging data were retrieved and archived for review using Digital Imaging and Communications in Medicine (DICOM) data transfer.

## 2.3 | Histopathological diagnosis

Biopsy samples and tumor resections collected at surgery at referral centers were fixed in 10% neutral-buffered formalin and shipped to the laboratory. After gross inspection, samples were trimmed in longitudinal and transverse orientation, and subjected to paraffin-embedding and sectioning. Whenever margins and orientation of resected tissue were marked by the submitting surgeon, sections of distal and proximal margins were sampled and followed the same paraffin-embedding and sectioning protocol. All slides were stained with hematoxylin-eosin (H&E), as well as Giemsa stain according to standard protocols. Immunohistochemistry for selected markers including, but not limited to S100, vimentin, glial fibrillary acidic protein (GFAP), and smooth muscle actin (SMA) was requested only if investigating pathologists (KM, MR) deemed doing so necessary to reach the final diagnosis of PNST.

Histopathology slides from all tumors were reviewed and graded, applying diagnostic algorithms adapted from a modified French

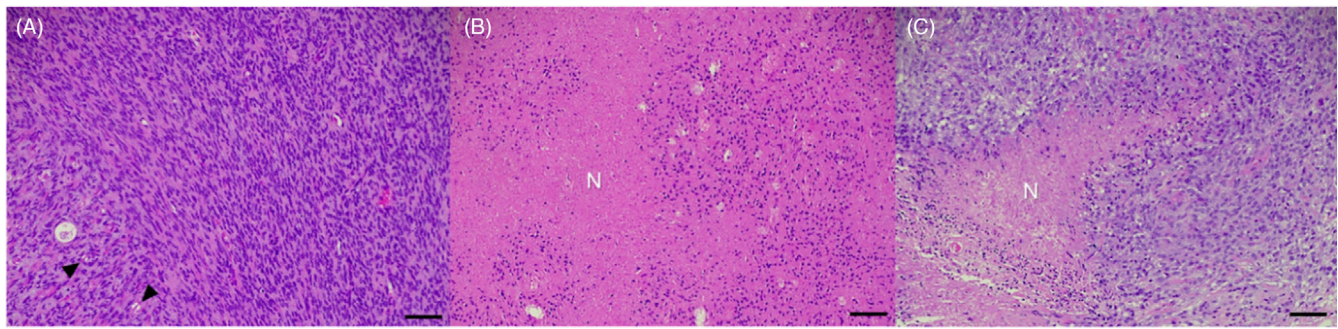


**FIGURE 1** Photomicrographs representative of the 3° of malignancy from grade 1 (Schwannoma) to grade 3 (MPNST) stained with Hematoxylin & Eosin (H&E) scale bar 50  $\mu$ m. Grade 1 (A) diffuse proliferation of well differentiated spindle cells among few recognizable axons (black arrowhead). Grade 2 (B) despite being still well differentiated proliferating cells show wide areas of necrosis (indicated by N). Grade 3 (C) moderate to marked pleomorphism of proliferating cells accompanied by necrosis and inflammation observed in lower left corner.

system (Fédération Nationale des Centres de Lutte Contre Le Cancer, FNCLCC) for grading human<sup>26</sup> and canine peripheral nerve sheath tumors<sup>7</sup> for relevant morphologic features<sup>5,27</sup> by a board-certified veterinary pathologist (MR). The score is reported in Table 1 and an example of the different grades is depicted in Figure 1.

In summary, tumors were histologically graded as grade 1 (score 2-3), grade 2 (score 4-5), or grade 3 (score 6-8) according to histological features of malignant behavior. Additional semi-quantitative scoring of morphologic features included amount of stroma, cystic changes, myxoid changes, inflammation, hemorrhage, pigments, calcification, tumor margins (positive with tumor cell infiltration; negative without tumor cell infiltration), and epineurial invasion (Table 1).

The relationship between individual histologic and MR features and tumor grade were assessed one-by-one to identify imaging findings predictive of tumor malignancy.

## 2.4 | Magnetic resonance imaging

Two board-certified radiologists reviewed all of the MRI studies (PD and SS) blinded to the grade of the tumor. The final decision on the imaging characteristics was reached by consensus. The studies were randomly reviewed using a DICOM viewer program (OsiriX DICOM viewer, version 8.0.2, Pixmeo, Geneva, Switzerland). The 2 observers were asked to fill in a pre-defined standardized commercially available spreadsheet (Microsoft Excel 2020, Microsoft, Redmond, Wash).

The MRI scanning techniques were similar for each institution. The coil selection was based on individual patients and availability at the institution. The MRI studies were obtained with both low- (2 of 0.3 Tesla, 1 of 0.25 Tesla, 1 of 0.4 Tesla and 3 of 0.18 Tesla) and high-field (4 of 3 Tesla and 3 of 1.5 Tesla) MRI scanners (Table S1). All MRI studies but 1 included at least T2W and T1W sequences before and after IV administration of 0.5 mL/kg of gadoteric acid. In 1 case, no precontrast T1w sequence was available. A short tau inversion recovery (STIR) sequence was available in 38/44 (86.3%) dogs.

The MRI characteristics of the lesions evaluated are presented in Table 2.

To reduce the number of statistical variables, the intradural and extradural portions were grouped as intracanal and the foraminal and paravertebral portions were grouped as peripheral (Figure 3); this approach also was needed because in some cases the correct differentiation between intradural and extradural was not possible because of the use of low-field magnetic resonance. The PNST volume was calculated using the OsiriX “closed polygon” tool by the first author in all but 2 cases using the T1 post-contrast sequence, 1 in the STIR with slice thickness from 2 to 2.5 mm. When available, T1 post-contrast 3-dimensional (3D) sequences were used (16/44, 36.3%) with slice thicknesses ranging from 0.9 to 2 mm. In 1 case it was not possible to obtain the volume because of the absence of DICOM images. The region of interest (ROI) was marked on all transverse slices from the most cranial to the most caudal part of the lesion. Then the “ROI/ROI volume/Compute volume” tool was used to calculate the volume of the lesion by summing the volumes of all of the ROIs of all the slices.

## 2.5 | Statistical analyses

Data were recorded and stored in an electronic spreadsheet (Microsoft Excel, version 2010; Microsoft Corporation, Redmond, Washington, USA). Commercial statistical software STATA (StataCorp. LLC. 2017. Stata Statistical Software: Release 15. College Station, Texas, USA) was used for all coding and statistical analysis. Continuous variables (eg, dog age, body weight, tumor volume) were assessed for normality of distribution using the Shapiro-Wilk test alongside visual assessment of histograms with overlaid kernel density plots. Normally distributed data were summarized using mean ( $\pm$ SD) and non-normally distributed data were summarized using median, interquartile range (IQR) and range. Categorical data were summarized as proportions and expressed as percentages.

The relationship between tumor grade and categorical variables of interest relating to histological diagnosis and MRI findings were assessed using Fisher's exact test. The Kruskal-Wallis test was used to



**TABLE 2** Standardized grading scheme for MRI criteria used in the study.

Location and extension of the tumor (cervical tract; brachial plexus; thoracolumbar tract; lumbar plexus)
Portion of the nerve affected: intracanal (intradural or epidural), peripheral (foraminal and paravertebral tracts) or a combination of the two
Number of peripheral nerves with changes (n.)
Volume (cm <sup>3</sup> )
Shape of the tumor in cross-section (rounded, fusiform, mass)
Presence of "dumbbell shape": the outward growth of an intracanal mass through the intervertebral foramen.
Margination (well-defined or unclear)
Evaluation of the foramina: complete obliteration of the foramina or persistent presence of fat around the foramina
Widening of the foramina (Yes/No)
Lysis of the bone (Yes/No)
Muscular atrophy (Yes/No) and grade (absent; mild; moderate; strong)
Signal intensity on various MRI pulse sequences
Contrast enhancement: intensity (absent; mild; moderate; strong) and distribution (homogenous; peripheral; central).
Presence of a cystic portion (Yes/No)
Presence of necrosis (Yes/No)
Internal fat component. (Yes/No)
Presence of fat split sign <sup>28</sup> : It is seen as a fine ring of fat around the lesion in human medicine. It is best appreciated in T1W images. (Yes/No)
Fascicular sign <sup>28</sup> : in human medicine, it is characterized by multiple, small, ring-like structures with peripheral hyperintensity and hypointense center in T2 representing the fascicular bundles within the nerves (Yes/No)
Presence of the target sign <sup>28</sup> : in human medicine, it represents a T2 hyperintense rim surrounding a central area of low signal (it is believed to be because of a dense central area of collagenous stroma) (Yes/No)

determine relationships between tumor grade and continuous variables (eg, dog age, dog weight, tumor volume). Where a potential relationship was initially identified ( $P < .1$ ) by the Kruskal-Wallis test, it was followed up using a post-hoc Dunn's test (with Sidák adjustment) to identify pair-wise relationships. Additionally, relationships between tumor grade and signalment (eg, dog age, body weight, sex) were assessed in a similar fashion to identify any potentially confounding factors or interactions.

$P$ -values  $< .05$  were considered significant.

### 3 | RESULTS

Forty-four cases met the inclusion criteria. Breeds represented in the study included Labrador retriever ( $n = 9$ ), cross-breeds ( $n = 8$ ), West Highland White Terrier ( $n = 3$ ), Jack Russell Terrier ( $n = 2$ ), Border Terrier ( $n = 2$ ), Beagle ( $n = 2$ ), Border Collie ( $n = 2$ ), Miniature Pinscher, American Staffordshire Terrier, Staffordshire Bull Terrier, Golden Retriever, Cavalier King Charles Spaniel, Fox Terrier, Magyar Vizsla, Doberman, Breton, Shi Tzu, Poodle, Magyar Vizsla, Yorkshire Terrier, Chihuahua, Coton de Tulear and Alaskan Malamute ( $n = 1$  each). Of the 44 dogs, 30 were males (68.1%), of which 6/30 (20%) were spayed, and 14 were females (31.8%), of which 9/14 (64.2%) were spayed. The median age of the dogs was 9 years (IQR, 7-11 years; range, 2-13 years) and the median weight was 20 kg (IQR, 13-30 kg; range, 4-40 kg).

Dogs were referred because of lameness (20/44), paraparesis (8/44), tetraparesis (4/44), monoparesis (4/44), hemiparesis (4/44),

ataxia (2/44), inability to jump (1/44), cervical hyperesthesia (1/44) and with the neurological examination were localized in the cranial cervical tract (11/44), cervicothoracic tract (18/44), thoracolumbar tract (4/44) and lumbosacral tract (11/44).

Tumor grade was not found to be associated with dog age (Kruskal-Wallis  $P$ -value, .67), body weight (Kruskal-Wallis  $P$ -value, .27) or sex (Fisher's exact  $P$ -value, .64).

#### 3.1 | Pathologic findings

Of the 44 samples submitted for histopathologic investigation 26 involved nerve roots and 18 the plexuses. Twenty-six were tumor resections and 18 were biopsy specimens. In 16/26 resections, sample orientation was provided and surgical margins were evaluated free of sampling biases and resulting in identification of positive margins with tumor cell infiltration in 15/16 (93.7%) and negative margins in 1/16 (6.2%). Overall, 16/44 (36.3%) of PNSTs were Grade 1, 19/44 (43.1%) Grade 2, and 9/44 (20.4%) Grade 3. Results of histopathologic examination are summarized in Table 3. Tumor grade was found to be associated with stroma formation, hemorrhage, presence of mineralization, and epineurial invasion and extension into the surrounding soft tissues.

The amount of stroma progressively increased with tumor grade, being present in 56.3% of Grade 1, 79.0% of Grade 2, and 100.0% of Grade 3 tumors ( $P = .05$ ).

Hemorrhage affecting  $< 50\%$  of tumor section (score 1) was present in 50.0% of Grade 1, 84.2% of Grade 2, and 100.0% of Grade

**TABLE 3** Histologic features sorted by tumor grading according to the modified diagnostic algorithms adapted from a modified French system (Fédération Nationale des Centres de Lutte Contre Le Cancer, FNCLCC) for soft tissue sarcomas in 44 dogs with confirmed PNST.

	Score	Grade 1 (n = 16)	Grade 2 (n = 19)	Grade 3 (n = 9)	Fisher's exact P-value
Hemorrhage	0	8 (50.0%)	3 (15.8%)	0 (0.0%)	.01*
	1	8 (50.0%)	16 (84.2%)	9 (100.0%)	
Amount of stroma	1	7 (43.8%)	4 (21.1%)	0 (0.0%)	.05*
	2	9 (56.3%)	15 (79.0%)	9 (100.0%)	
Myxoid change	0	9 (56.3%)	8 (42.1%)	2 (22.2%)	.26
	1	3 (18.8%)	7 (36.8%)	6 (66.6%)	
	2	4 (25.0%)	4 (21.1%)	1 (11.1%)	
Cystic change	0	13 (81.3%)	17 (89.5%)	8 (88.9%)	.85
	1	3 (18.8%)	2 (10.5%)	1 (11.1%)	
Mineralization	0	16 (100.0%)	11 (57.9%)	9 (100.0%)	.001*
	1	0 (0.0%)	8 (42.1%)	0 (0.0%)	
Inflammation	0	6 (37.5%)	7 (36.8%)	4 (44.4%)	.67
	1	6 (37.5%)	8 (42.1%)	5 (55.6%)	
	2	4 (25.0%)	4 (21.1%)	0 (0.0%)	
Pigments	0	14 (87.5%)	17 (89.5%)	9 (100.0%)	.82
	1	2 (12.5%)	2 (10.5%)	0 (0.0%)	
Margins	Negative	3 (18.8%)	1 (5.3%)	0 (0.0%)	.32
	Positive	13 (81.3%)	18 (94.7%)	9 (100.0%)	
Epineurial invasion	0	8 (50.0%)	1 (5.3%)	0 (0.0%)	.002*
	1	8 (50.0%)	18 (94.7%)	9 (100.0%)	

\* $P < .05$ .

3 tumors ( $P = .01$ ). Tumor mineralization was present in a subset (42.1%) of Grade 2 PNSTs and was not identified in Grade 1 or Grade 3 tumors ( $P = .001$ ). Invasion of the epineurium by neoplastic cells and extending into the surrounding soft tissues progressively increased in frequency along with increasing tumor grade (50% of Grade 1 tumors, 94.7% of Grade 2, and 100.0% of Grade 3 tumors;  $P = .002$ ).

Significant relationships between tumor grade and the remaining morphologic features were not identified.

### 3.2 | Magnetic resonance imaging

The brachial plexus (C6-T2) was commonly affected (18/44, with 6/16 of grade 1, 5/19 of grade 2, and 7/9 of grade 3), followed by the cervical tract (C1-C5; 11/44, with in 4/16 of grade 1, 6/19 of grade 2, and 1/9 of grade 3) and lumbar plexus (L4-S3; 11/44, with 5/16 of grade 1, 6/19 of grade 2, and 0/9 of grade 3). The thoracolumbar tract (T3-L3) was the least common site (4/44, with 1/16 of grade 1, 2/19 of grade 2, 1/9 of grade 3; Figure 2A).

Most PNSTs involved both the intracanal and peripheral compartment, particularly grade 1 and grade 2. None of the grade 3 tumors involved only the intracanal tract (Figure 2B). Only 8/44 (18.1%) cases had a dumbbell shape (Figure 3).

The MRI findings of the different grades and of the PNSTs are presented in Table 4.

In general, PNSTs had overlapping imaging findings despite distinct histologic grades. Grade 3 PNSTs had larger volume (median, 4.18 cm<sup>3</sup>; IQR, 0.97-33.69 cm<sup>3</sup>) compared to grade 1 tumors (median, 0.97 cm<sup>3</sup>; IQR, 0.37-2.04 cm<sup>3</sup>;  $P = .03$ ) although tumor volume was not significantly different between grade 1 and grade 2 tumors nor between grade 2 and grade 3 tumors (Figure 4).

On T1 post-contrast studies, grade 1 and 2 tumors had the highest frequency of homogenous distribution of contrast medium (75.0% and 84.2%, respectively) and grade 3 the lowest (37.5%;  $P = .04$ ; Figure 5A,B,D,E). Conversely, grade 3 tumors had the highest frequency of peripheral distribution (62.5%) and it was lower in grade 1 (18.8%) and grade 2 (10.5%) tumors (Figure 5C,F).

Two cases showed intracanal and peripheral locations with contrast enhancement only in the intracanal component and not the peripheral component (Figure 6). The intensity of the contrast enhancement was strong in 12/16 grade 1, 12/19 grade 2, and 4/9 grade 3 tumors; it was moderate in 2/16 grade 1, 4/12 grade 2, and 1/8 grade 3; and mild in 2/16 grade 1, 3/19 grade 2, and 3/8 grade 3 tumors. Significant relationships between tumor grade and the remaining MRI features were not identified.

The internal fat component was not included in the statistical analysis because of lack of consistent sequences from MRI protocols

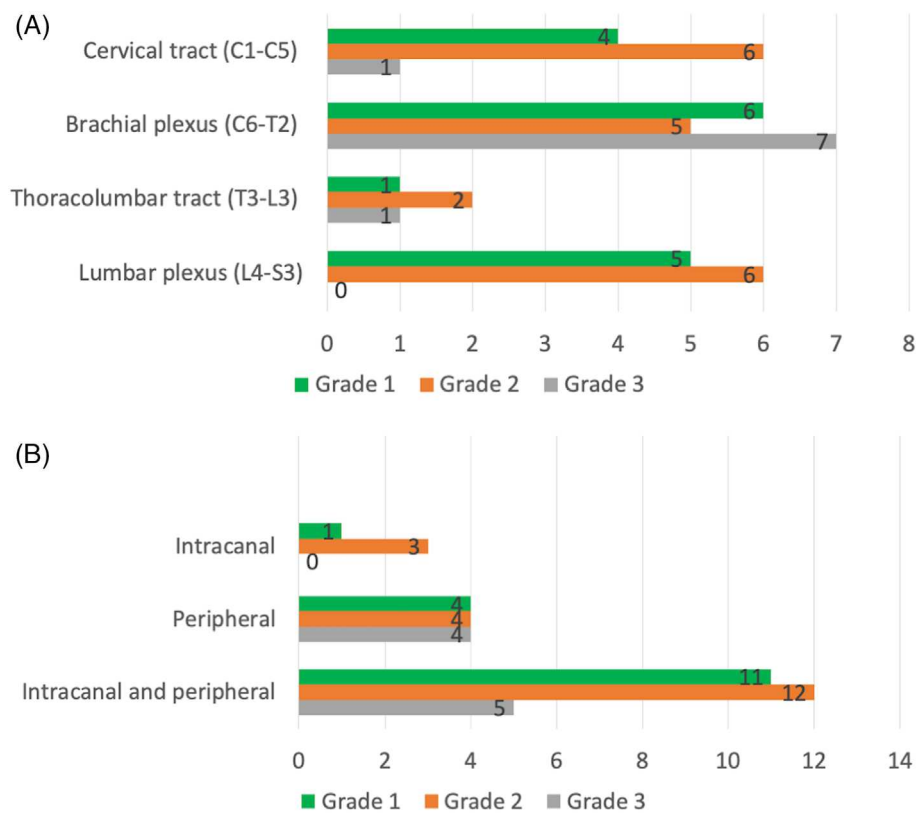


**FIGURE 2** (A) Distribution of the peripheral nerve sheath tumors along the spinal cord. (B) Tract of the nerve affected.

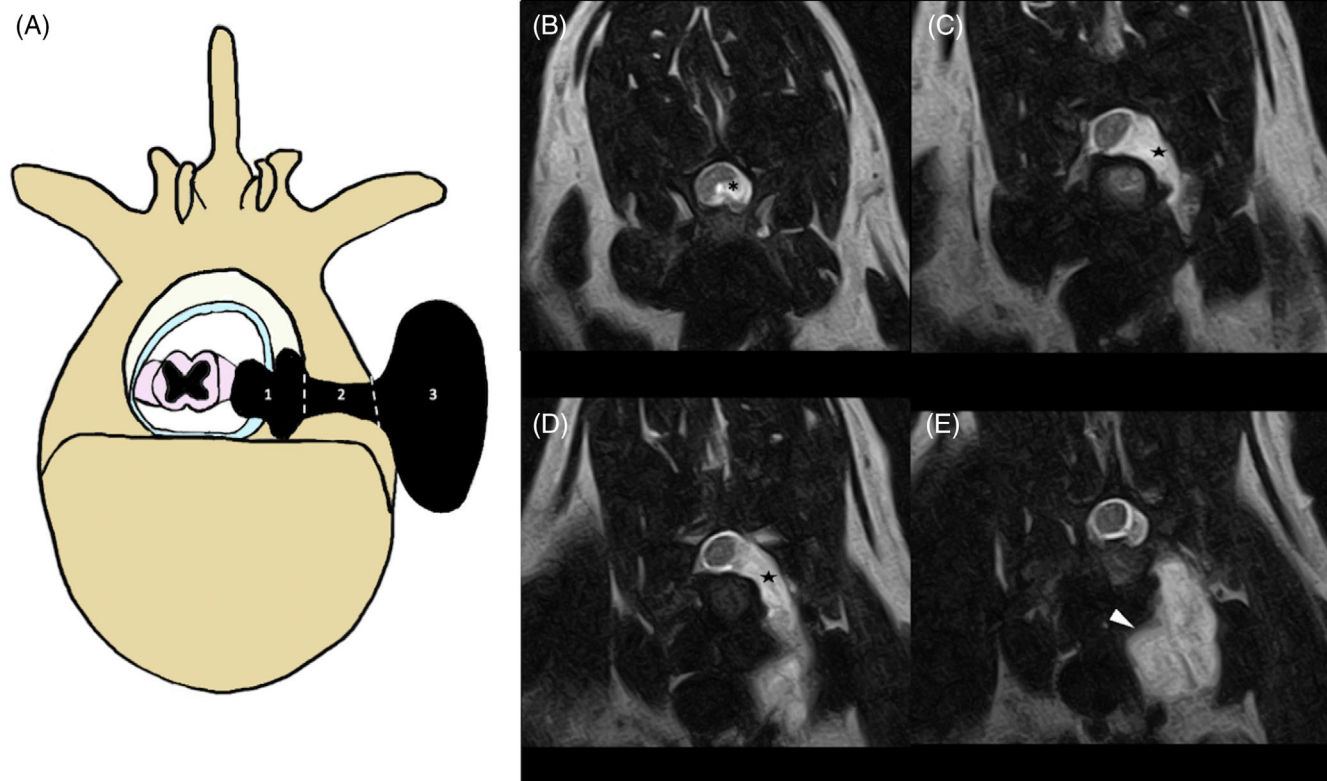


**FIGURE 3** Graphical representation of the different components of a PNST (A) and sequential slices of the MRI in the same dog with a peripheral nerve sheath tumor affecting the brachial plexus (B-E); in this case a combination of components is noted: in (B) intracanal portion (asterisk), in (C-D) peripheral/foraminal (star) and (E) peripheral/paravertebral (head of arrow). In (A): intracanal (1), peripheral/foraminal (2), peripheral/paravertebral (3).



**TABLE 4** Standardized grading scheme for magnetic resonance imaging (MRI) criteria used in 44 dogs with confirmed PNST.

	Score	Grade 1 (n = 16)	Grade 2 (n = 19)	Grade 3 (n = 9)	P
Numbers of nerve	1	10 (62.5%)	16 (84.2%)	6 (66.7%)	.35
	2	3 (18.8%)	3 (15.8%)	2 (22.2%)	
	3	3 (18.8%)	0 (0.0%)	1 (11.1%)	
Shape	Mass	0 (0.0%)	2 (10.5%)	2 (22.2%)	.18
	Rounded	2 (12.5%)	6 (31.6%)	1 (11.1%)	
	Tubular	14 (87.5%)	11 (57.9%)	6 (66.7%)	
Margins	Well-defined	12 (75.0%)	17 (89.5%)	8 (88.9%)	.56
	Unclear	4 (25.0%)	2 (10.5%)	1 (11.1%)	
Foramen and fat obliteration	No	2 (12.5%)	6 (31.6%)	4 (44.4%)	.23
	Yes	14 (87.5%)	13 (68.4%)	5 (55.6%)	
Enlargement of the foramen with bone atrophy	No	2 (12.5%)	6 (31.6%)	2 (22.2%)	.42
	Yes	14 (87.5%)	13 (68.4%)	7 (77.8%)	
Dumbbell shape**	Yes	3 (18.75%)	4 (21.05%)	1 (11.1%)	1
	No	13 (81.25%)	15 (78.95%)	8 (88.8%)	
Muscle atrophy***	No	3 (18.8%)	1 (5.6%)	0 (0.0%)	.33
	Yes	13 (81.3%)	17 (94.4%)	9 (100.0%)	
Grade atrophy	None	3 (18.8%)	1 (5.6%)	0 (0.0%)	.73
	Mild	4 (25.0%)	8 (44.4%)	5 (55.6%)	
	Moderate	5 (31.3%)	5 (27.8%)	2 (22.2%)	
	Strong	4 (25.0%)	4 (22.2%)	2 (22.2%)	
Signal intensity in T1	Hyperintense	2 (13.3%)	3 (16.7%)	0 (0.0%)	.70
	Isointense	13 (86.7%)	15 (83.3%)	8 (100.0%)	
Signal intensity in T2	Hyperintense	14 (87.5%)	14 (73.7%)	9 (100.0%)	.49
	Hypointense	1 (6.3%)	1 (5.3%)	0 (0.0%)	
	Isointense	1 (6.3%)	4 (21.1%)	0 (0.0%)	
Signal intensity in STIR	Hyperintense	14 (100.0%)	14 (93.3%)	9 (100.0%)	1.00
	Isointense	0 (0.0%)	1 (6.7%)	0 (0.0%)	
Heterogeneity of the signal in T1	No	15 (100.0%)	16 (88.9%)	7 (87.5%)	.41
	Yes	0 (0.0%)	2 (11.1%)	1 (12.5%)	
Heterogeneity of the signal in T2	No	8 (50.0%)	9 (47.4%)	4 (44.4%)	1.00
	Yes	8 (50.0%)	10 (53.6%)	5 (55.6%)	
Contrast intensity	Mild	2 (12.5%)	3 (15.8%)	3 (37.5%)	.63
	Moderate	2 (12.5%)	4 (21.1%)	1 (12.5%)	
	Severe	12 (75.0%)	12 (63.2%)	4 (50.0%)	
Distribution of contrast medium	Homogenous	12 (75.0%)	16 (84.2%)	3 (37.5%)	.05*
	Intracanal	1 (6.3%)	1 (5.3%)	0 (0.0%)	
	Peripheral	3 (18.8%)	2 (10.5%)	5 (62.5%)	
Cystic portion	No	16 (100.0%)	19 (100.0%)	7 (87.5%)	.19
	Yes	0 (0.0%)	0 (0.0%)	1 (12.5%)	
Necrosis	No	14 (87.5%)	13 (68.4%)	5 (55.6%)	.23
	Yes	2 (12.5%)	6 (31.6%)	4 (44.4%)	
Fat split sign	No	12 (75.0%)	11 (57.9%)	8 (44.4%)	.32
	Yes	4 (25.0%)	8 (42.1%)	5 (55.6%)	

\*P &lt; .05. \*\*30 dogs included.

\*\*\*1 of grade 2 was not available (amputation of the affected limb).

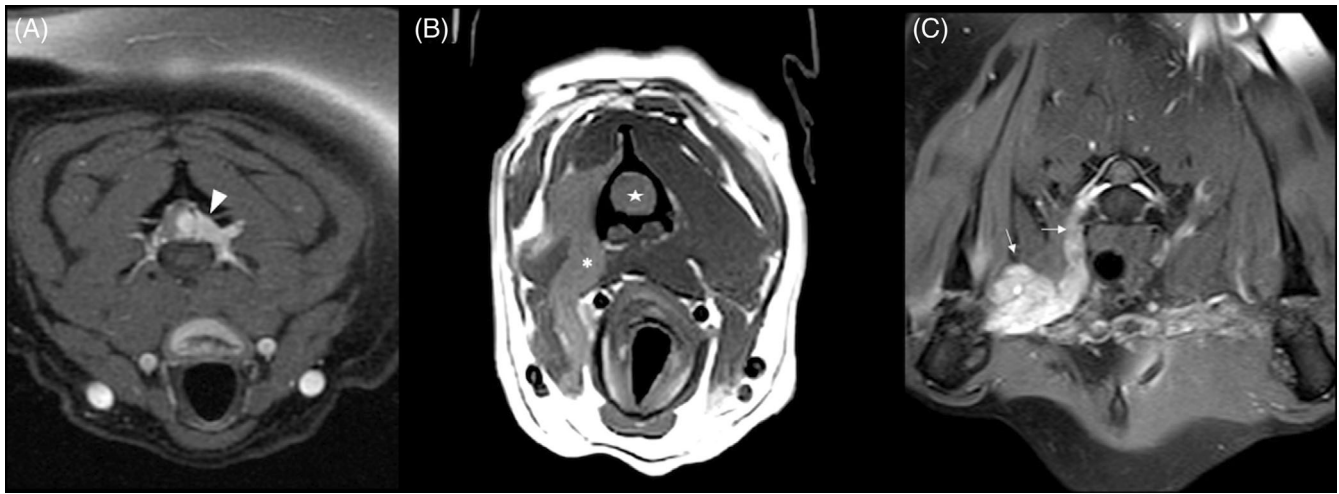


**FIGURE 4** Representation of the different size of the PNSTs based on grade: Grade 1 (A): transverse section of T1W fat sat post contrast at the level of the cervical spinal of an intracanal and left foraminal PNST (small size); Grade 2 (B): transverse section of T1W contrast at the level of the cervical spinal of an intracanal, right foraminal and peripheral PNST (medium size); Grade 3 (C): transverse view of T1W fat sat post contrast at the level of the brachial plexus of a peripheral mass aspect PNST (large size).

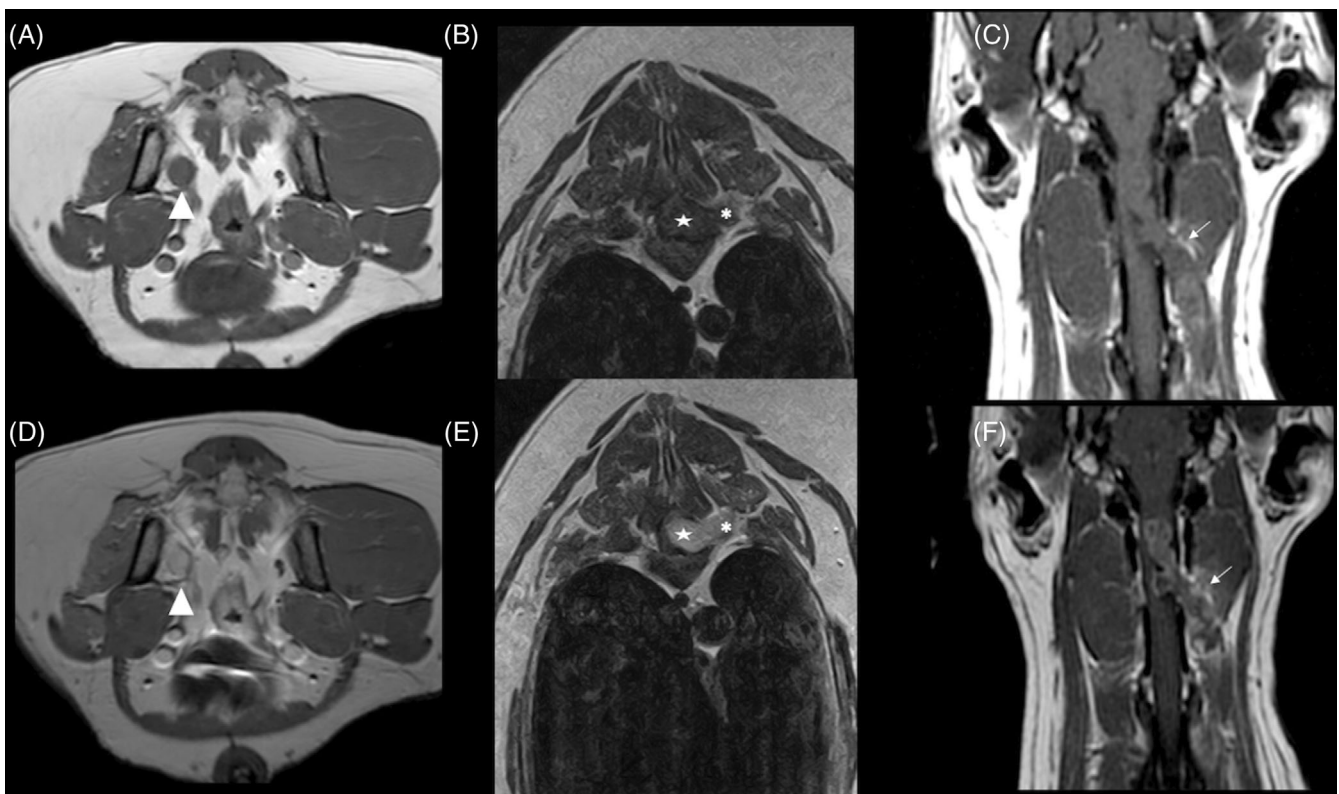


**FIGURE 5** Representation of the different enhancement of PNSTs based on grade: Grade 1 (A-D): transverse section of T1W pre contrast (A) and T1w post contrast (D) at the level of the pelvic canal of peripheral tract of PNST (white head of arrow) affecting the right sciatic nerve with homogenous contrast enhancement; Grade 2 (B-E): transverse section of T1W pre-contrast (B) and T1W post-contrast (E) at the level of the thoracolumbar tract of an intracanal (star), left foraminal and peripheral (asterisk) PNST with homogenous contrast enhancement; Grade 3 (C-F): dorsal section of T1W pre-contrast (C) and T1W post-contrast (F) at the level of the cervical spinal of an intracanal, left foraminal and peripheral PNST with peripheral contrast enhancement (arrow).

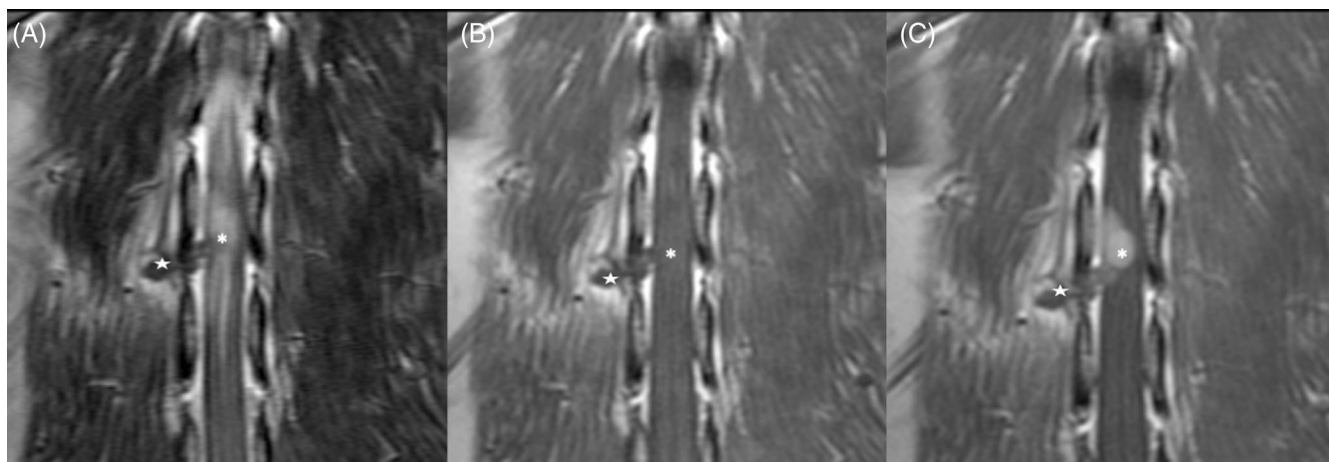


**FIGURE 6** Different enhancement of the PNST based on the tract: intracanal and peripheral PNST in dorsal T2W (A), T1W pre-contrast (B), and T1W post-contrast (C) with enhancement of the intracanal portion without enhancement of the peripheral part.

necessary to evaluate these findings. Fascicular and target signs, described in human patients,<sup>26</sup> were excluded because of the absence of consensus on these findings.

## 4 | DISCUSSION

We analyzed the MRI features of PNSTs and their relationship with histological grade to identify imaging features predictive of malignancy. We found that different malignancy grades of PNSTs shared several MRI features. However, some qualitative MRI characteristics were significantly associated with the grade of PNSTs such as large tumor volume and distribution of contrast enhancement. Large tumor volume was significantly associated with high tumor grade. In contrast, homogenous contrast enhancement was significantly associated with tumors of low grade, whereas peripheral contrast enhancement was most consistently reported in high-grade tumors.

In our cohort of patients, grade 3 tumors were significantly larger than grade 1. In human medicine, tumor size is a discriminating factor between benign and malignant PNSTs and 5 cm in diameter is used as cut-off.<sup>28</sup> Rapid growth in malignant tumors is probably the reason behind this size dichotomy<sup>29</sup> and it likely reflects a more rapid onset and progression of clinical signs compared with low-grade tumors. Despite wider variations in the overall size of dogs compared to humans, we still could appreciate a significant contribution of tumor size to grade prediction and prognosis. As a general rule, the size of soft tissue sarcomas and the anatomic location impact the feasibility of complete surgical excision and tumor-free margins.<sup>30</sup> Large tumor size generally is considered a poor predictive factor for surgery and radiotherapy.<sup>31</sup>

In our study, homogenous contrast enhancement was significantly associated with tumors of low grade (grade 1), whereas peripheral contrast enhancement was most consistently reported in high-grade tumors (grade 2). In humans, peripheral enhancement is noted in malignant PNSTs, and central focal enhancement is observed

in their benign counterparts.<sup>29,32</sup> Most likely, the degree of differentiation of benign tumors from normal tissue is such that proliferated cells and supporting fibrovascular stroma grow at a similar rate resulting in homogeneous growth of new tissue. The opposite might occur in high-grade tumors where cell proliferation, metabolic demand and nutritional and oxygen supply are out of balance as demonstrated by tumor necrosis and hemorrhage. According to previous studies in people,<sup>33,34</sup> peripheral enhancement also may reflect poor central vascularization and increased compactness of the tumor. Decreased extracellular space and abnormal vascular changes can result in thrombosis, hemorrhage, necrosis, and cyst formation.<sup>33</sup> Histopathology identified substantially increased frequency of intra-tumoral hemorrhage and amount of stroma deposition in high-grade PNSTs that would explain differences of contrast distribution among grades.

Enhancement of the intracanal compartment of the tumor without enhancement of the peripheral part was observed in 2 cases. This characteristic may be related to the absence of invasion of the tumor within the foraminal tract of the nerve, and the distal thickening of the nerve could be caused by edema from compression of the intradural mass. This hypothesis also may explain the thickening of >1 nerve that we observed.

In our cases, the brachial plexus was the most commonly affected site, particularly for high grade PNSTs because no grade 3 was encountered in the lumbar plexus. This result is in agreement with previous literature where few case reports described lumbosacral location of PNSTs.<sup>6,35</sup>

Surprisingly, no correlation was identified between spinal cord compression and grade of malignancy.

Grade 1 and grade 2 tumors mainly involved the intracanal compartments, whereas grade 3 mostly affected the peripheral segment of the spinal nerves. Regardless, the finding may not correlate with better prognosis, because gross tumor margins are difficult to identify on visual inspection during surgical procedures, and involvement of neighboring nerves or nerve roots limits the chance of complete resection within the space of the vertebral canal.<sup>15</sup>

Tubular shape on MRI was the most common imaging finding of PNSTs independent of grade according to previous studies in both humans<sup>29</sup> and veterinary patients.<sup>15</sup> However, in our cases, only grade 2 and grade 3 had a mass-like appearance whereas in grade 1 a mass-like appearance was not observed. Regardless of the shape associated with more benign grades in our cohort, elongated shape and anatomic contiguity of a space occupying lesion adjacent to peripheral nerves and nerve roots is considered highly suggestive of PNST.<sup>36</sup>

The term “dumbbell-shape” applies to a group of tumors arising along the vertebral column featuring 1 part of the tumor inside the spinal canal and the other part in the paravertebral space connected with each other by a portion of tumor traversing the neural foramen.<sup>37</sup> In our study, few cases (8/44, 18.1%) had this feature and no correlation was found with tumor grade.

In our cases, no relationship was found between ill-defined margins on MRI studies and high-grade tumors. In recent human medical literature, benign PNSTs had with well-defined margins, whereas malignant PNSTs had a tendency toward ill-defined margins or had an abnormal signal intensity relative to adjacent soft tissue.<sup>36</sup> Other authors considered these 2 features manifestations of aggressive neuroinvasive lesions, including malignant tumors, but other etiologies such as infectious or inflammatory lesions could not be reliably ruled out.<sup>21</sup> Microscopic assessment of margin invasion did not identify correlations between positive invaded margins and tumor grade in our study, possibly reflecting anatomic restrictions to complete surgical resection rather than providing further information on tumor grade, behavior or both.

In humans, malignant PNST can cause lysis of the vertebrae, and this finding appears to correlate with grade of malignancy. In our study, none of the tumors caused detectable lysis of adjacent vertebrae on MRI, as previously reported in veterinary medicine.<sup>17</sup> However, we observed mild bony changes consistent with pressure atrophy of the affected vertebrae (34/44, 77.2%). Pressure atrophy is a consequence of local impairment of blood supply resulting in thinning and rarefaction of bones in contrast to osteolysis derived from neoplastic infiltration and substitution of bone tissue.

Muscle atrophy is a frequently described secondary change that has been associated with PNSTs and it is reported in 23% of affected human patients.<sup>16</sup> On the contrary, other soft tissue tumors only rarely are accompanied by muscle atrophy and compression or constriction of the peripheral or central nervous system is required to induce such changes. Chronic denervation of the target organ from motor nerve fiber loss adds to disuse of the affected limb, ultimately resulting in muscle atrophy.<sup>18</sup> For some body areas and skeletal muscles, such as those innervated by the brachial plexus, volumetric changes can be subtle and may require measurements and comparison with the normal, clinically unaffected, side to become evident. For this reason, and concordance with previous literature,<sup>15</sup> we recommend increasing the size of the field of view (FOV) by starting the MRI examination with the dorsal plane in order to visualize a large portion of axial and upper appendicular skeletal muscles for side comparison. In our study, muscle atrophy was a frequent finding (40/44), ranging from mild to severe but showed no correlation with tumor grade.

According to a previous study,<sup>15</sup> T2- and T1-weighted (W) pre- and post-contrast pulse sequences were essential for PNSTs detection. In our study and according to the previous study, the STIR sequence was necessary because it increased the radiologist's ability to identify the affected nerves, suppressing signal from fat and making the hyperintense neoplastic lesions more noticeable.<sup>15</sup> The STIR was available in 38/44 (86.3%) cases and it was used as the first sequence to decrease the time for identifying the nerve changes, because it is a fat-suppressing technique with high sensitivity for fluid and pathology<sup>37</sup> and it was particularly useful in studies when low-field MR is used, in which spectral fat suppression is not possible.<sup>38</sup>

The “fat split-sign” (a fine ring of fat signal surrounding the bulk of the tumor) is a radiologic sign reported in radiology in human medicine and it is correlated with benign behavior because of the lack of infiltration of surrounding tissues. It is best appreciated on the peripheral nerves, such as the distal portion of the brachial or lumbar plexus, when cleavage is present between tumor and soft tissues. None of the patients in our study had the “fat split-sign”, which might be because of overrepresentation of high-grade tumors as well as higher frequency of PNSTs location within the vertebral canal or the foraminal tract. Nevertheless, radiologists should be aware of this sign and look for it.

Fascicular and target signs described in human patients<sup>28</sup> were excluded from analysis because of the absence of consensus among radiologists on these findings. These signs have never been described in veterinary medicine and there was no confidence in their identification between radiologists. The fascicular sign is detectable on T2W MRI images and is characterized by multiple small ring-like structures with peripheral hyperintensity representing bundles of nerve fibers within the peripheral nerves. The target sign consists of a central area of low intensity surrounded by a T2W hyperintense rim. Both signs correlate with benign tumor behavior according to the human medical literature,<sup>28</sup> but according to our observations, they appear to be of little value for grade prediction.

As a retrospective multi-center study, our study had some limitations. Because both low- and high-field MRI equipment was used in the study and the protocols were not standardized, it was not possible to differentiate among extradural, intradural and intramedullary location in some cases. Detection of hemorrhage, necrosis, cystic lesions, and metaplastic changes that contribute to establishing tumor grade also was also impaired for the same reason. The lack of the gradient sequence (T2\*W and susceptibility weighted imaging [SWI]), the gold standard for detecting hemorrhage and venous structures,<sup>39</sup> and fluid-attenuated inversion recovery (FLAIR), the gold standard for detecting cystic lesions,<sup>40</sup> might have decreased the sensitivity of image analysis for further characterizing these specific changes and decreasing the capacity to identify a correlation between high tumor grade and the presence of necrosis, cystic lesion, and a hemorrhagic component. Hence, implementation of T2\*W, SWI, and FLAIR sequences should be considered and tested in prospective studies for clarification of their contribution to radiographic prediction of tumor grade. Another limitation relates to on the composition of the studied PNSTs being clearly skewed toward high-grade tumors, that might have limited detection and description of imaging features typical of



low-grade tumors. This result might simply reflect the natural selection of patients from secondary and tertiary referral centers for neurosurgical procedures and specialized neuropathology evaluation.

In conclusion, MRI provides features predictive of high-grade PNSTs including tumor size and peripheral contrast enhancement that might better guide patient management in terms of surgical planning and ancillary treatments. Introduction of a grading system for PNSTs in dogs in larger prospective studies ultimately will provide useful information on the prognostic utility of such a system, response to different treatments, disease progression and overall survival.

#### ACKNOWLEDGMENT

No funding was received for this study.

#### CONFLICT OF INTEREST DECLARATION

Luisa De Risio is employed by Linnaeus veterinary limited, a provider of veterinary services. No other authors declare a conflict of interest.

#### OFF-LABEL ANTIMICROBIAL DECLARATION

Authors declare no off-label use of antimicrobials.

#### INSTITUTIONAL ANIMAL CARE AND USE COMMITTEE (IACUC) OR OTHER APPROVAL DECLARATION

Approved by the Research Ethics Committee of the Animal Health Trust (Ref19/2019).

#### HUMAN ETHICS APPROVAL DECLARATION

Authors declare human ethics approval was not needed for this study.

#### ORCID

Simona Morabito  <https://orcid.org/0000-0001-6148-4000>

Luisa De Risio  <https://orcid.org/0000-0001-9005-4165>

João Ribeiro  <https://orcid.org/0000-0003-2472-2895>

Katrin Beckmann  <https://orcid.org/0000-0002-1823-7845>

Thomas Flegel  <https://orcid.org/0000-0001-9892-0224>

Marco Rosati  <https://orcid.org/0000-0002-1485-1610>

#### REFERENCES

- May W. MRI of the brachial and lumbosacral plexuses. In: May W, ed. *Diagnostic MRI in Dogs and Cats*. 1st ed. Taylor & Francis Ltd, Boca Raton; 2018:603-617.
- Sirri R, Sabattini S, Bettini G, Mandrioli L. Reclassification of 21 presumptive canine peripheral nerve sheath tumours (PNST) using a literature-based immunohistochemical panel. *Acta Veterinaria-Beograd*. 2016;66:455-465.
- Chijiwa K, Uchida K, Tateyama S. Immunohistochemical evaluation of canine peripheral nerve sheath tumours and other soft tissue sarcomas. *Vet Pathol*. 2004;41:307-318.
- Lanigan LG, Russel DS, Woolard KD, et al. Comparative pathology of the peripheral nervous system. *Vet Pathol*. 2021;58:10-33.
- WHO Classification of Tumours Editorial Board. Central nervous system tumours. *WHO classification of tumours series*. Vol 6. 5th ed. Lyon (France): International Agency for Research on Cancer; 2021.
- Abraham LA, Mitten RW, Beck C, et al. Diagnosis of sciatic nerve tumour in two dogs by electromyography and magnetic resonance imaging. *Aust Vet J*. 2002;81:39-40.
- Tekavec K, Švara T, Knific T, Gombač M, Cantile C. Histopathological and immunohistochemical evaluation of canine nerve sheath tumors and proposal for an updated classification. *Vet Sci*. 2022;9:204.
- Hansen KS, Zwngenberg AL, Théon AP, et al. Treatment of MRI-diagnosed trigeminal peripheral nerve sheath tumors by stereotactic radiotherapy in dogs. *J Vet Intern Med*. 2016;40:1112-1120.
- Brehm AM, Vite CH, Steinberg H, et al. A retrospective evaluation of 51 cases of peripheral nerve sheath tumours in the dogs. *J Am Anim Hosp Assoc*. 1995;31:349-359.
- Angelov L, Davis A, O'Sullivan B, Bell R, Guha A. Neurogenic sarcomas: experience at the University of Toronto. *Neurosurgery*. 1998;43:56-64.
- Wanebo JE, Malik JM, VandenBerg SR, et al. Malignant peripheral nerve sheath tumors. A clinicopathologic study of 28 cases. *Cancer*. 1993;71:1247-1253.
- Gross TL, Ihrke PJ, Walder EJ, et al. Neural and perineural tumors. In: Gross TL, Ihrke PJ, Walder EJ, Affolter VJ, eds. *Skin Diseases of the Dog and Cat: Clinical and Histopathologic Diagnosis*. 2nd ed. Wiley-Blackwell, Oxford; 2005:789-796.
- Yao X, Zhou H, Dong Y, et al. Malignant peripheral nerve sheath tumors: latest concepts in disease pathogenesis and clinical management. *Cancer*. 2023;15:1-19.
- Rudich SR, Feeney DA, Anderson KL, Walter PA. Computed tomography of masses of the brachial plexus and contributing nerve roots in dogs. *Vet Rad Ultrasound*. 2004;45:46-50.
- Kraft S, Ehrhart EJ, Gall D, et al. Magnetic Resonance imaging characteristics of peripheral nerve sheath tumours of the canine brachial plexus in 18 dogs. *Vet Radiol Ultrasound*. 2007;48:1-7.
- Platt SR, McConnel F. What is your diagnosis? Malignant nerve sheath tumour. *J Small Anim Pract*. 2002;43:39-40.
- Platt SR, Graham J, Chrisman CL, et al. Magnetic resonance imaging and ultrasonography in the diagnosis of a malignant peripheral nerve sheath tumour in a dog. *Vet Radiol Ultrasound*. 1999;40:367-371.
- Anderson O, Langley-Hobbs SJ. A peripheral nerve sheath tumour in the median nerve of a dog. *Vet Record Case Report*. 2022;10:e323. doi:10.1002/vrc2.323
- Lacassagne K, Hearon K, Berg J, et al. Canine spinal meningiomas and nerve sheath tumours in 34 dogs (2008-2016): distribution and long-term outcome based upon histopathology and treatment modality. *Vet Comp Oncol*. 2018;16:344-351.
- Matsuda M, Ikeda S, Sakurai S, et al. Hypertrophic neuritis due to chronic inflammatory demyelinating polyradiculoneuropathy (CIDP): a postmortem pathological study. *Muscle Nerve*. 1996;19:163-169.
- Stumpo M, Foschini MP, Poppi M, Cenacchi G, Martinelli P. Hypertrophic inflammatory neuropathy involving bilateral brachial plexus. *Surg Neurol*. 1999;52:458-464.
- Rodenas S, Summers BA, Saverald T, et al. Chronic hypertrophic ganglioneuritis mimicking spinal nerve neoplasia: clinical, imaging, pathologic findings, and outcome after surgical treatment. *Vet Surg*. 2013;42:91-98.
- Soderlund V, Goranson H, Bauer HC. MR imaging of benign peripheral nerve sheath tumors. *Acta Radiol*. 1994;35:282-286.
- Pilavaki M, Chourmouzi D, Kiziridou A. Imaging of peripheral nerve sheath tumors with pathologic correlation: pictorial review. *Eur J Radiol*. 2004;52:229-239.
- McCarville MB. What MRI can tell us about neurogenic tumors and rhabdomyosarcoma. *Pediatr Radiol*. 2016;46:881-890.
- Rodríguez FJ, Al F, Giannini C, et al. Pathology of peripheral nerve sheath tumors: diagnostic overview and update on selected diagnostic problems. *Acta Neuropathol*. 2012;123:295-319.
- Chikkannaiah P, Boovalli MM, Nathiyal V, Venkataramappa S. Morphological spectrum of peripheral nerve sheath tumors: an insight into World Health Organization 2013 classification. *J Neurosci Rural Pract*. 2016;7:346-354.
- Kakkar C, Shetty CM, Koteshwara P, Bajpai S. Telltale signs of peripheral neurogenic tumours on magnetic resonance imaging. *Indian J Radiol Imaging*. 2015;25:453-458.



29. Yu Y, Wu J, Ye J, Chen MX. Radiological findings of malignant peripheral nerve sheath tumor: reports of six cases and review of literature. *World J Surg Oncol*. 2016;10:142.
30. Dernell WS, Withrow SJ, Kuntz CA, Powers BE. Principles of treatment for soft tissue sarcoma. *Clin Tech Small Anim Pract*. 1998;13:59-64.
31. Dennis MM, McSparran KD, Bacon NJ, et al. Prognostic factors for cutaneous and subcutaneous soft tissue sarcomas in dogs. *Vet Pathol*. 2011;48:73-84.
32. Ogose A, Hotta T, Morita T, et al. Tumors of peripheral nerves: correlation of symptoms, clinical signs, imaging features, and histologic diagnosis. *Skeletal Radiol*. 1999;28:183-188.
33. Friedman DP, Tartaglino LM, Flanders AE. Intradural meningiomas of the spine: MR findings with emphasis on contrast-enhancement characteristics. *AJR Am J Roentgenol*. 1992;158:1347-1350.
34. Sze G, Bravo S, Krol G. Spinal lesions: quantitative and qualitative temporal evolution of gadopentetate dimeglumine enhancement in MR imaging. *Radiology*. 1989;170:849-856.
35. Da Silva Nêto Souza AC, da Costa Vieira Filho CH, Beanes Da Silva EM, et al. Lumbar malignant peripheral nerve sheath tumor in a young dog. *Acta Scientiae Veterinaria*. 2021;49:631.
36. Li CS, Huang GS, Wu HD, et al. Differentiation of soft tissue benign and malignant peripheral nerve sheath tumors with magnetic resonance imaging. *Clin Imaging*. 2008;32:121-127.
37. Konar M, Lang J. Pros and cons of low-field magnetic resonance imaging in veterinary practice. *Vet Radiol Ultrasound*. 2011;52:S5-S14.
38. Dennis R. Optimal magnetic resonance imaging of the spine. *Vet Radiol Ultrasound*. 2011;52:S72-S80.
39. Weston P, Morales C, Dunning M, et al. Susceptibility weighted imaging at 1.5 tesla magnetic resonance imaging in dogs: comparison with T2\*-weighted gradient echo sequence and its clinical indications. *Vet Radiol Ultrasound*. 2020;61:566-576.
40. Dickinson PJ, Jones-Woods S, Cissel DD. Abrogation of fluid suppression in intracranial postcontrast fluid-attenuated inversion recovery magnetic resonance imaging: a clinical and phantom study. *Vet Radiol Ultrasound*. 2018;59:432-443.

#### SUPPORTING INFORMATION

Additional supporting information can be found online in the Supporting Information section at the end of this article.

**How to cite this article:** Morabito S, Specchi S, Di Donato P, et al. Relationship between magnetic resonance imaging findings and histological grade in spinal peripheral nerve sheath tumors in dogs. *J Vet Intern Med*. 2023;37(6): 2278-2290. doi:[10.1111/jvim.16839](https://doi.org/10.1111/jvim.16839)